

Development of a magnetic 3D spheroid-based platform for high-throughput drug screening

Wei Mei Guo^a, Xian Jun Loh^b, Ern Yu Tan^c, Joachim S.C. Loo^d, Vincent H.B. Ho^{a,*}

^a*Molecular Engineering Laboratory, A*STAR, Proteos, 61 Biopolis Drive, Singapore 138673, Singapore*

^b*Institute of Materials Research and Engineering, A*STAR, 3 Research Link, Singapore 117602, Singapore*

^c*Department of General Surgery, Tan Tock Seng Hospital, 11 Jalan Tan Tock Seng, Singapore 308433, Singapore*

^d*School of Materials Science and Engineering, Nanyang Technological University, 50 Nanyang Avenue, Singapore 639798, Singapore*

* E-mail: vincehohb@gmail.com

Abstract

Three dimensional (3D) cell culture has become increasingly adopted as a more accurate model of the complex *in vivo* microenvironment compared to conventional two dimensional (2D) cell culture. Multicellular spheroids are important 3D cell culture models widely used in biological studies and drug screening. To facilitate simple spheroid manipulation, cells were magnetically labeled using a scaffold-free approach to generate magnetic spheroids. This method is applicable to a variety of cell types. The spheroids generated can be targeted and immobilized using magnetic field gradients, allowing media change or dilution to be performed with minimal disruption to the spheroids. The cells in magnetic spheroids showed good viability and displayed typical 3D morphology. Using this platform, a 28 day study was carried out using doxorubicin on magnetic MCF-7 spheroids. The results provided a proof-of-principle for using magnetic tumor spheroids in therapeutic studies and demonstrated additional insights into cellular behaviour that were not apparent in 2D monolayer assays. Furthermore, this platform can be modified for high-throughput screening in drug discovery.

Keywords: multicellular spheroids; magnetic cell labeling; spheroid manipulation; therapeutic studies; high-throughput screening

1. Introduction

In recent years, there has been increasing emphasis on three dimensional (3D) cell culture systems. This is due to the increase in demand for more physiologically-relevant *in vitro* tissue models which can recapitulate the actual *in vivo* conditions [1-3]. These models provide more clinically relevant results in preclinical studies [4, 5]. Two dimensional (2D) cell cultures have been commonly employed for evaluating efficacy or toxicity of drug candidates in screening studies. However, studies have shown that there are significant differences in the phenotypic and functional characteristics when cells are grown in monolayers or 3D cultures [6-8]. The 2D environment poorly reflects the complex 3D *in vivo* microenvironment where cells are in close contact with other cell types and the extracellular matrix, and are subject to cellular interactions that influence cell differentiation, proliferation and migration [9].

Multicellular spheroids (MCS) are a simple and widely used 3D cell culture system. They are usually formed by spontaneous aggregation and fusion of cells without any external artificial scaffolds [10-12]. Homotypic MCS can be obtained from a broad range of cell types. Different cell types can also be co-cultured to create heterotypic MCS [13, 14]. These microtissues exhibit high similarities to actual tissues in features such as cellular heterogeneity, nutrient and oxygen gradients, matrix deposition and cell-cell signaling [15]. MCS also offer the opportunity for prolonged studies as they can be cultured for weeks in contrast to cells grown in monolayers which will be over-confluent in a matter of days [16, 17].

Various approaches have been established to generate 3D spheroids. Conventional methods include spinner flask or liquid overlay culture [18, 19] while others have utilized protein [20] or synthetic polymer scaffolds [21, 22]. There are more advanced spheroid formation methods which include micron-scaled substrates [23] and microfluidic devices [24, 25]. Although these offer certain advantages such as higher throughput of spheroid generation or simplified liquid handling, some of these systems are complicated and require sophisticated equipment and specialized training.

The hanging drop culture allows precise control over spheroid size and uses readily available laboratory substrates. Recently, it was shown that spheroids in hanging drops could be magnetically manipulated by introducing magnetic labels into the

spheroids [14]. This methodology was then applied in tissue engineering and drug screening. However, it was recognized that the hanging drop method might not be compatible with automated handling for higher throughput applications without further substrate modification [26, 27].

In this study, a platform consisting of magnetic microtissues for drug screening is developed. It provides a simple methodology for manipulating 3D spheroids on a larger scale. Various human cell lines were magnetically labeled using a previously described method. Labeled cells were then seeded into low attachment 96-well micro plates for spheroid generation [28]. The magnetic spheroids cultured from labeled cells could be manipulated with magnetic field gradients. This facilitates complete media change with minimal disruption to the spheroids and reduces spheroid loss. Imaging of the microtissues can be carried out using conventional microscopy or automated cell imager. An Food and Drug Administration (FDA)-approved drug was used as a model drug for screening studies using this platform.

2. Experimental Section

2.1 Materials

Biotinamidohexanoic acid N-hydroxysuccinimide ester (BiotinSE, Sigma B2643), 366 mM in DMSO, was stored at -20°C . Streptavidin MagneSpheres paramagnetic particles (Promega Z5482), 1 mg mL^{-1} , were stored at 4°C . Dulbecco's Phosphate Buffered Saline (PBS, PAA H15-002) was stored at room temperature. CellTiter-Blue® (Promega G8081) was stored at 4°C . *p*-nitrophenyl phosphate disodium salt hexahydrate (Sigma N9389) was stored at -20°C .

2.2 Cell culture

MCF-7 human breast adenocarcinoma cells were grown in Dulbecco's Modified Eagle's Medium (DMEM, Gibco 11965) supplemented with 10% fetal bovine serum, 100 U mL^{-1} penicillin and $100\text{ }\mu\text{g mL}^{-1}$ streptomycin. The cells were cultured in a 5% CO_2 humidified atmosphere at 37°C .

2.3 Spheroid culture

MCF-7 cells were magnetically labeled using a previously established method [29]. Briefly, the cells were treated with $750\mu\text{M}$ BiotinSE in PBS at room temperature for

30 min. Biotinylated cells were added to 0.025 mg mL^{-1} streptavidin paramagnetic particles and vortexed at room temperature for 15s to ensure uniform mixing of cells and particles. To generate magnetic MCF-7 spheroids, 100 μL medium containing 500 magnetically labeled cells were dispensed into wells of 96-well round bottom low attachment plate (Corning Inc. 7007). The spheroids were cultured in a 5% CO_2 humidified atmosphere at 37°C .

2.4 Drug treatment

The diameter size of the spheroid used for 3D studies was $\sim 400\mu\text{m}$. The spheroids were washed with PBS after the plate was placed on a 96-Well Magnetic Separator (Invitrogen CS15096) to direct the spheroids to the side of the well. The spheroids were then resuspended by removing the separator and incubated with or without doxorubicin at various concentrations: 0.01, 0.1, 1, 10, 100 $\mu\text{g mL}^{-1}$, prepared in medium. The spheroids were incubated at 37°C for 24 h before the drugs were removed. They were washed with PBS and fresh media was supplemented before further culture of up to 28 days with media change every 2 days.

2.5 Confocal microscopy

MCF-7 spheroids were stained with 20 μM fluorescein dicacetate and 25 $\mu\text{g/mL}$ propidium iodide for 2 h at 37°C . They were then placed on 35 mm glass-bottom culture dishes (MatTek) and imaged using a Zeiss LSM 5 DUO confocal laser scanning microscope. Both dyes were excited using the 488 nm laser line. Z-stacks were taken until the fluorescence was lost. These images were then compiled into 3D projections.

2.6 F-actin staining

MCF-7 cells and spheroids were fixed in 4% paraformaldehyde (ChemCruz™ SC-281692) for 30 min and permeabilized with 0.5% Triton X-100 (Promega H5142) diluted in DPBS for 15 min. F-actin was stained with Rhodamin phalloidin (Invitrogen R415) (15 μL methanolic stock solution diluted in 600 μL 0.1% BSA in PBS) for 20 min. Cell nuclei were counterstained with Hoechst 33342 (Invitrogen H3570) for 10 min. All treatments were carried out at room temperature.

2.7 Growth monitoring

The size of the spheroids was measured by taking images of the spheroid using an inverted phase contrast microscope (Zeiss AXIOVERT 40 CFL). The spheroid size was determined from measurements of two orthogonal diameters from which the geometric mean diameter was calculated [16].

2.8 Histology

MCF-7 spheroids were fixed with 10% neutral buffered formalin for 2 h at 4°C and washed with PBS. The fixed spheroids were prepared using a VIP tissue processor (Sakura, Japan). The process consisted of dehydration in a series of increasing ethanol concentrations up to 100% and then two changes of xylene and four changes of paraffin wax (Paraplast) and eventual embedding in paraffin. The duration for each step is 10 min. Spheroid sections were cut at 5 µm thickness and stained with haematoxylin and eosin. Stained sections were imaged using a Nikon AZ 100 microscope.

2.9 Quantitative Real-time Polymerase Chain Reaction (qRT-PCR)

Total RNA was isolated from MCF-7 spheroids using Trizol® Reagent (Invitrogen 15596-028) with Purelink™ RNA Mini Kit (Invitrogen 12183-018A). 200 ng of total RNA was reverse transcribed into complementary DNA (cDNA) using Superscript™ III First-strand synthesis system for qRT-PCR (Invitrogen 18080-051). qRT-PCR was performed using the StepOnePlus™ Real-Time PCR Systems (Applied Biosystems) and the amplifications were done using Maxima SYBR Green/ROX qPCR master mix (2×) (Fermentas, K0221). The thermal cycling conditions were composed of initial denaturation step at 95°C for 5 min, followed by 45 cycles at 95°C for 10 s, 57°C for 15 s and 60°C for 50 s. The experiments were carried out in triplicate for each data point and a standard curve was included. Data was normalized to that of 2D MCF-7 cell monolayer. GAPDH was used as the housekeeping gene. The sequences for the primers are:

VEGF-A 5'-CTG CTG TCT TGG GTG CAT TGG-3' (Forward)

5'-TCA CCG CCT CGG CTT GTC-3' (Reverse)

GAPDH 5'-AAGGTGAAGGTCGGAGTCAA-3' (Forward)

5'-GAAGATGGTGATGGGATTTC-3' (Forward)

2.10 Acid phosphatase assay

Using the 96-well Magnetic Separator, the spheroids were directed to the side of the well, the supernatant were carefully removed and replaced with 100 μ L PBS. 100 μ L of the assay buffer (0.1M sodium acetate, 0.1% TritonX-100, supplemented with (mass?)*p*-nitrophenyl phosphate, Sigma N9389) was added to each well and incubated for 90 min at 37°C. Following incubation, 10 μ L of 1N sodium hydroxide (NaOH) was added, and absorption at 405 nm was measured using a Tecan Infinite 200 microplate reader (reference).

3. Results and discussion

3.1 Generation and manipulation of magnetic multicellular spheroids

To generate magnetic multicellular spheroids for screening, single cells labeled with paramagnetic particles were seeded into round-bottomed wells of low attachment 96-well microplates. The labeled cells aggregated at the bottom of the well and formed a compact magnetic spheroid over time. The method of cell labeling was based on affinity interaction. It involved biotinylation of the cell membrane proteins followed by conjugation to the streptavidin paramagnetic particles. This stepwise method was quick; it did not require cellular internalization of particles. Uptake of magnetic particles varied in different cell types and required an incubation period up to 24 hours [30-32]. Figure 1 shows how spheroids are generated and can be manipulated to one end of the well using a magnet array placed under the plate. There was minimum disturbance to the immobilized spheroid during fluid withdrawal and allowed for culture medium exchange or addition of drugs with lower risk of spheroid loss. As a demonstration of the adaptive application of this method, uniformly-sized magnetic multicellular spheroids were successfully generated from a range of non-tumor and tumor cell lines (Figure 2).

3.2 Structural characteristics of magnetic multicellular spheroids

F-actin cytoskeletal organization in 2D monolayer MCF-7 cells and magnetic MCF-7 spheroids were observed using confocal microscopy by Rhodamin phalloidin staining. In 2D MCF-7 cells (Figure 3A), stress fibers were observed to spread throughout the cytoplasm. This shows evidence of cell adhesion to the substrate they are grown on. Figure 3B showed a cortical F-actin network typical of 3D cell morphology and proved that there was cytoskeletal reorganization when cells self-assembled into 3D

spheroid. The formation of intercellular interactions in 3D spheroids closely resembled the actual *in vivo* tissue environment.

The cell viability in the spheroids was assessed using a live/dead stain in confocal microscopy. Viable cells were stained green due to the conversion of fluorescein diacetate to fluorescein by intercellular esterases, while non-viable cells that lost membrane integrity were stained red by propidium iodide. As shown in Figure 3C, the majority of the cells within the 7-day-old spheroid were viable. There was a significant increase in the number of non-viable cells in the 14-day-old spheroid (Figure 3D). Establishment of a diffusion gradient in larger 3D multicellular structures likely limited nutrient and oxygen delivery to cells at the centre of the spheroids, leading to hypoxia and consequent necrosis.

Histological analysis of hematoxylin and eosin (H&E) stained sections of the magnetic MCF-7 spheroids revealed the morphological characteristics of individual cells arranged in a densely packed morphology (Figure 3E). It was also shown that cells were aggregated together with the paramagnetic particles within the spheroid (insert white arrows to point to particles in the figure). Very few dead cells observed, demonstrating that the particles were not toxic to the cells. Spheroids cultured for a much longer time were observed to have a more concentric cellular arrangement with cells in the core appearing necrotic (Figure 3F). This further verified the observation above that mass transport limitations in spheroid caused cell death in spheroid core [33]. Notably, the paramagnetic particles remained present within the older spheroid and were not lost.

3.3 Gene expression profiles of 3D multicellular spheroids

Gene expression level of vascular endothelial growth factor (VEGF-A), a classic marker for hypoxia stress [34] was investigated (Figure 4). Quantitative PCR was conducted using RNA from 2D and 3D cell samples. Spheroids cultured for 4 days have VEGF-A expression patterns similar to those from 2D monolayers. Relative expression of VEGF-A was up-regulated in spheroids cultured for nine days and became elevated significantly by day 14 of prolonged cultures. These data further

supported the evidence of hypoxia-induced necrosis observed in the H&E histology staining in Figure 3F.

3.4 Long-term culture of 3D multicellular spheroids

The ease of culture medium exchange using magnetic manipulation is promising for long-term spheroid culture. Figure 5 shows prolonged culture of spheroids of more than 5 weeks, and was possible because media change could be carried out with ease and repeatedly on the same plate with minimal spheroid interference. The use of 96-well plates allows one to upscale the platform to facilitate efficient high-throughput drug screening. It provides the opportunity of continuous observation and quantitative analysis of spheroid culture in prolonged therapeutic studies with durations comparable to animal studies.

3.5 Establishment of 3D spheroid-based assay for therapeutic screening

The 96-well microplate format was employed in this study (Figure 6) to develop a platform for standardized spheroid culturing, rapid imaging and analysis that was amenable to large-scale drug screening. The low attachment property of the microplate provided a non-adherent surface that prevents cell adhesion. The round bottom well shape promoted the formation of reproducible and homogeneously sized spheroids. A water reservoir was constructed around the periphery of the microplate to prevent a commonly encountered problem where medium near the edges are more prone to evaporation (reference. Vinci et al?). The use of microplates is compatible with existing high-throughput screening systems. Measurement of the growth kinetics of the spheroids in response to the drug can be carried out using conventional microscopy or automated cell imager. In this study, a benchtop *in situ* cellular analysis system – Celigo™ cytometer (Brooks Life Science System) was used. This cytometer scans a 96-well plate within ten minutes. Bright field images were acquired and analyzed. Growth curves of the multicellular spheroids can be rapidly and easily generated from the multi-parametric data analysis, which includes measurements of spheroid diameter, perimeter and area.

3.6 Drug treatment of 3D multicellular spheroids

Doxorubicin, a conventional anticancer drug was used as a model drug for therapeutic studies using 3D spheroids. Magnetic MCF-7 tumor spheroids of $\sim 400\ \mu\text{m}$ in diameter were exposed to free doxorubicin for 24 hours before further culture of 28 days, similar to the length of animal studies. The culture medium was exchanged every 48 hours using the method described above. Monitoring of drug effect on spheroid integrity and volume growth was analyzed and plotted in Figure 7A. The graph showed a dose-dependent response of the MCF-7 spheroids to doxorubicin. Spheroid growth inhibition and evident cell shedding occurred with drug treatment at concentration of $1\ \mu\text{g mL}^{-1}$ and above. Recovery from growth inhibition was observed at drug concentration of $0.1\ \mu\text{g mL}^{-1}$ and below after 14 days. Acid phosphatase assay was performed to analyze spheroid viability at the study endpoint [19, 35]. The assay result showed a similar dose-dependent effect where a gradual drop in spheroid viability resulted from increasing doxorubicin concentration (Figure 7B). These results showed that magnetic 3D tumor spheroids could be used in drug efficacy testing.

4. Conclusion

In this study, magnetic multicellular spheroids were generated from magnetically labeled cells using 96-well round bottom low attachment plate. The methodology can be applied to a wide variety of cell types for spheroid generation. Morphological analysis of the spheroids revealed good cell viability and structural characteristics commonly observed in 3D tissue structures. The magnetic labeling of cells provides a facile method to manipulate the 3D spheroids with transiently applied magnetic fields. This is convenient for medium exchange and can support long-term culturing. The platform developed provides a simple and versatile method of screening therapeutic candidates against tumor spheroids, and is particularly valuable when seeking to evaluate the efficacy in prolonged preclinical studies. It offers a more realistic model than 2D cell monolayer and has the potential to be modified for higher throughput systems.

Acknowledgements

The authors would like to thank both Singapore Biomedical Research Council, Agency for Science, Technology and Research (BMRC, A*STAR) and National Medical Research Council, Ministry of Health (NMRC, MOH) for funding support. Histology images were acquired in the SBIC-Nikon Imaging Centre at Biopolis, Singapore.

References

1. Griffith LG, Swartz MA. Capturing complex 3D tissue physiology in vitro. *Nature reviews Molecular cell biology*. 2006;7(3):211-24.
2. Rimann M, Graf-Hausner U. Synthetic 3D multicellular systems for drug development. *Current opinion in biotechnology*. 2012;23(5):803-9.
3. Pampaloni F, Reynaud EG, Stelzer EH. The third dimension bridges the gap between cell culture and live tissue. *Nature reviews Molecular cell biology*. 2007;8(10):839-45.
4. Smalley KS, Lioni M, Herlyn M. Life isn't flat: taking cancer biology to the next dimension. *In vitro cellular & developmental biology Animal*. 2006;42(8-9):242-7.
5. Nyga A, Cheema U, Loizidou M. 3D tumour models: novel in vitro approaches to cancer studies. *Journal of cell communication and signaling*. 2011;5(3):239-48.
6. Kim JB. Three-dimensional tissue culture models in cancer biology. *Seminars in cancer biology*. 2005;15(5):365-77.
7. Kunz-Schughart LA, Freyer JP, Hofstaedter F, Ebner R. The use of 3-D cultures for high-throughput screening: the multicellular spheroid model. *Journal of biomolecular screening*. 2004;9(4):273-85.
8. Friedrich J, Ebner R, Kunz-Schughart LA. Experimental anti-tumor therapy in 3-D: spheroids--old hat or new challenge? *International journal of radiation biology*. 2007;83(11-12):849-71.
9. Kimlin LC, Casagrande G, Virador VM. In vitro three-dimensional (3D) models in cancer research: an update. *Molecular carcinogenesis*. 2013;52(3):167-82.
10. Achilli TM, Meyer J, Morgan JR. Advances in the formation, use and understanding of multi-cellular spheroids. *Expert opinion on biological therapy*. 2012;12(10):1347-60.
11. Hirschhaeuser F, Menne H, Dittfeld C, West J, Mueller-Klieser W, Kunz-Schughart LA. Multicellular tumor spheroids: an underestimated tool is catching up again. *Journal of biotechnology*. 2010;148(1):3-15.
12. Lin RZ, Chang HY. Recent advances in three-dimensional multicellular spheroid culture for biomedical research. *Biotechnology journal*. 2008;3(9-10):1172-84.
13. Bratt-Leal AM, Kepple KL, Carpenedo RL, Cooke MT, McDevitt TC. Magnetic manipulation and spatial patterning of multi-cellular stem cell aggregates. *Integrative biology : quantitative biosciences from nano to macro*. 2011;3(12):1224-32.
14. Ho VH, Guo WM, Huang CL, Ho SF, Chaw SY, Tan EY, et al. Manipulating Magnetic 3D Spheroids in Hanging Drops for Applications in Tissue Engineering and Drug Screening. *Advanced healthcare materials*. 2013.
15. LaBarbera DV, Reid BG, Yoo BH. The multicellular tumor spheroid model for high-throughput cancer drug discovery. *Expert opinion on drug discovery*. 2012;7(9):819-30.
16. Ho VH, Muller KH, Barcza A, Chen R, Slater NK. Generation and manipulation of magnetic multicellular spheroids. *Biomaterials*. 2010;31(11):3095-102.

17. Mehta G, Hsiao AY, Ingram M, Luker GD, Takayama S. Opportunities and challenges for use of tumor spheroids as models to test drug delivery and efficacy. *Journal of controlled release : official journal of the Controlled Release Society*. 2012;164(2):192-204.
18. Friedrich J, Seidel C, Ebner R, Kunz-Schughart LA. Spheroid-based drug screen: considerations and practical approach. *Nature protocols*. 2009;4(3):309-24.
19. Wen Z, Liao Q, Hu Y, You L, Zhou L, Zhao Y. A spheroid-based 3-D culture model for pancreatic cancer drug testing, using the acid phosphatase assay. *Brazilian journal of medical and biological research = Revista brasileira de pesquisas medicas e biologicas / Sociedade Brasileira de Biofisica [et al]*. 2013;46(7):634-42.
20. Talukdar S, Mandal M, Hutmacher DW, Russell PJ, Soekmadji C, Kundu SC. Engineered silk fibroin protein 3D matrices for in vitro tumor model. *Biomaterials*. 2011;32(8):2149-59.
21. Loessner D, Stok KS, Lutolf MP, Hutmacher DW, Clements JA, Rizzi SC. Bioengineered 3D platform to explore cell-ECM interactions and drug resistance of epithelial ovarian cancer cells. *Biomaterials*. 2010;31(32):8494-506.
22. Fischbach C, Chen R, Matsumoto T, Schmelzle T, Brugge JS, Polverini PJ, et al. Engineering tumors with 3D scaffolds. *Nature methods*. 2007;4(10):855-60.
23. Markovitz-Bishitz Y, Tauber Y, Afrimzon E, Zurgil N, Sobolev M, Shafran Y, et al. A polymer microstructure array for the formation, culturing, and high throughput drug screening of breast cancer spheroids. *Biomaterials*. 2010;31(32):8436-44.
24. Shin CS, Kwak B, Han B, Park K. Development of an in vitro 3D tumor model to study therapeutic efficiency of an anticancer drug. *Molecular pharmaceutics*. 2013;10(6):2167-75.
25. Hsiao AY, Torisawa YS, Tung YC, Sud S, Taichman RS, Pienta KJ, et al. Microfluidic system for formation of PC-3 prostate cancer co-culture spheroids. *Biomaterials*. 2009;30(16):3020-7.
26. Hsiao AY, Tung YC, Qu X, Patel LR, Pienta KJ, Takayama S. 384 hanging drop arrays give excellent Z-factors and allow versatile formation of co-culture spheroids. *Biotechnology and bioengineering*. 2012;109(5):1293-304.
27. Tung YC, Hsiao AY, Allen SG, Torisawa YS, Ho M, Takayama S. High-throughput 3D spheroid culture and drug testing using a 384 hanging drop array. *The Analyst*. 2011;136(3):473-8.
28. Vinci M, Gowan S, Boxall F, Patterson L, Zimmermann M, Court W, et al. Advances in establishment and analysis of three-dimensional tumor spheroid-based functional assays for target validation and drug evaluation. *BMC biology*. 2012;10:29.
29. Ho VH, Muller KH, Darton NJ, Darling DC, Farzaneh F, Slater NK. Simple magnetic cell patterning using streptavidin paramagnetic particles. *Experimental biology and medicine*. 2009;234(3):332-41.
30. Kim JA, Choi JH, Kim M, Rhee WJ, Son B, Jung HK, et al. High-throughput generation of spheroids using magnetic nanoparticles for three-dimensional cell culture. *Biomaterials*. 2013;34(34):8555-63.
31. Souza GR, Molina JR, Raphael RM, Ozawa MG, Stark DJ, Levin CS, et al. Three-dimensional tissue culture based on magnetic cell levitation. *Nature nanotechnology*. 2010;5(4):291-6.

32. Whatley BR, Li X, Zhang N, Wen X. Magnetic-directed patterning of cell spheroids. *Journal of biomedical materials research Part A*. 2013.
33. Desoize B, Jardillier J. Multicellular resistance: a paradigm for clinical resistance? *Critical reviews in oncology/hematology*. 2000;36(2-3):193-207.
34. Kelm JM, Diaz Sanchez-Bustamante C, Ehler E, Hoerstrup SP, Djonov V, Ittner L, et al. VEGF profiling and angiogenesis in human microtissues. *Journal of biotechnology*. 2005;118(2):213-29.
35. Friedrich J, Eder W, Castaneda J, Doss M, Huber E, Ebner R, et al. A reliable tool to determine cell viability in complex 3-d culture: the acid phosphatase assay. *Journal of biomolecular screening*. 2007;12(7):925-37.

Figure captions

Figure 1. Schematic of generation and manipulation of magnetic spheroids in microplate format.

Cells are first labeled with paramagnetic particles and seeded in 96-well low attachment round bottom plates. Spheroids formed can be directed to the side of the wells by an external magnet. Upon spheroid immobilization, complete media change or addition of drug can be carried out for long term culture and drug treatment studies.

Figure 2. Homotypic magnetic spheroids generated from different cell lines.

Formation of magnetic spheroids from non-cancer cell lines (A-E) and cancer cell lines (F-K) in low attachment round bottom 96-well plates. (A) MCF10A, (B) HEK 293, (C) BEAS-2B, (D) human mesenchymal stem cells (hMSC), (E) BJ, (F) HeLa, (G) MDA-MB-231, (H) MCF-7, (I) HCT 116, (J) HepG2, and (K) A549. Scale bars represent 200 μm .

Figure 3. Structural and morphological characterization of magnetic spheroids.

F-actin visualization in (A) MCF-7 monolayer and (B) MCF-7 spheroid. Cell viability assay using fluorescein diacetate for staining viable cells and propidium iodide for non-viable cells. (C) 7 day-old spheroid. (D) 14 day-old spheroid. Hematoxylin-and-eosin staining of cross-sections of MCF-7 spheroids. (E) 7 day-old (F) 14 day-old.

Figure 4. Relative expression of vascular endothelial growth factor (VEGF-A) analyzed by RT-qPCR

The expression levels of vascular endothelial growth factor (VEGF-A) in 3D MCF-7 spheroid are shown relative to the expression level of VEGF-A genes in 2D MCF-7 monolayer cells.

Figure 5. Long-term culture of 3D magnetic spheroids.

Representative phase contrast images of magnetic MCF-7 spheroids cultured long term with complete media change continued once every two days. (A) 22 day (B) 30 day (C) 39 day.

Figure 6. 3D magnetic spheroid-based assay for therapeutic screening

Magnetic spheroids generated in 96-well plate were imaged using conventional microscopy or automated cell imager to capture spheroid integrity and volume following drug treatment. Spheroid analysis includes measurements of mean spheroid diameter to generate growth curves and frequency distribution curves. Monitoring of drug effects on spheroids was determined through the acid phosphatase (APH) assay to measure spheroid viability.

Figure 7. Effect of doxorubicin on volume growth and spheroid viability in 3D magnetic spheroid assay.

MCF-7 spheroids were treated with various concentration of doxorubicin for 24 h. The drug was removed and spheroids were further cultured for 28 days. Spheroid volume growth was monitored over the entire duration and spheroid viability was measured at the end of the study. Values are means \pm SD (n=10).

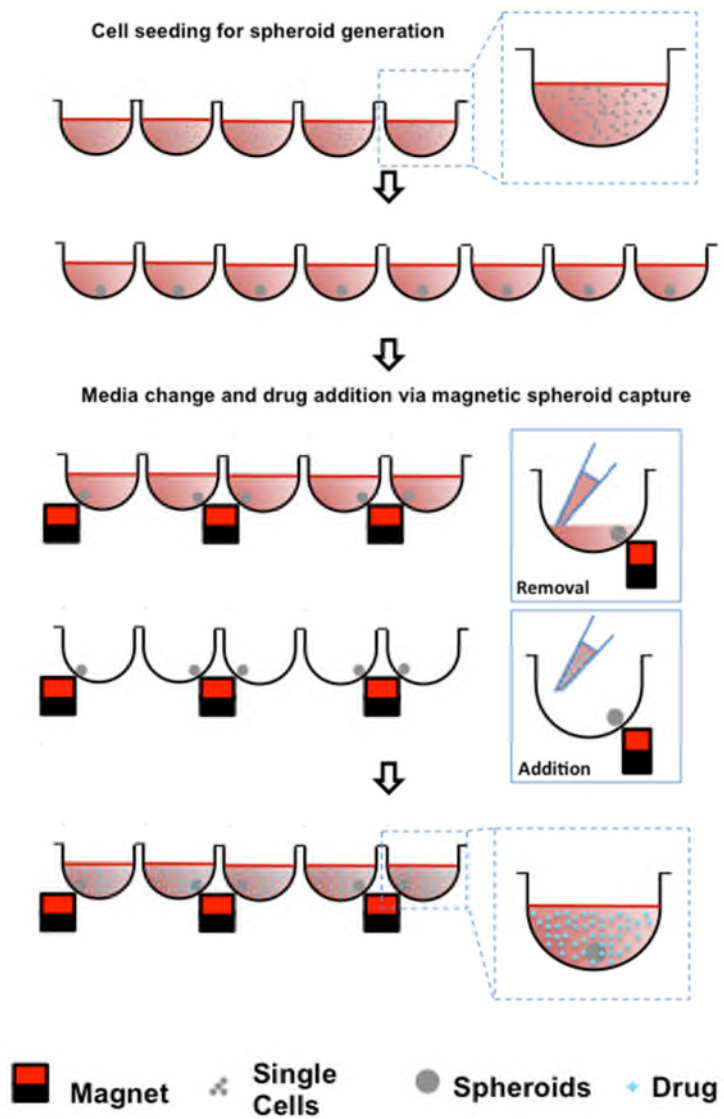


Figure 1

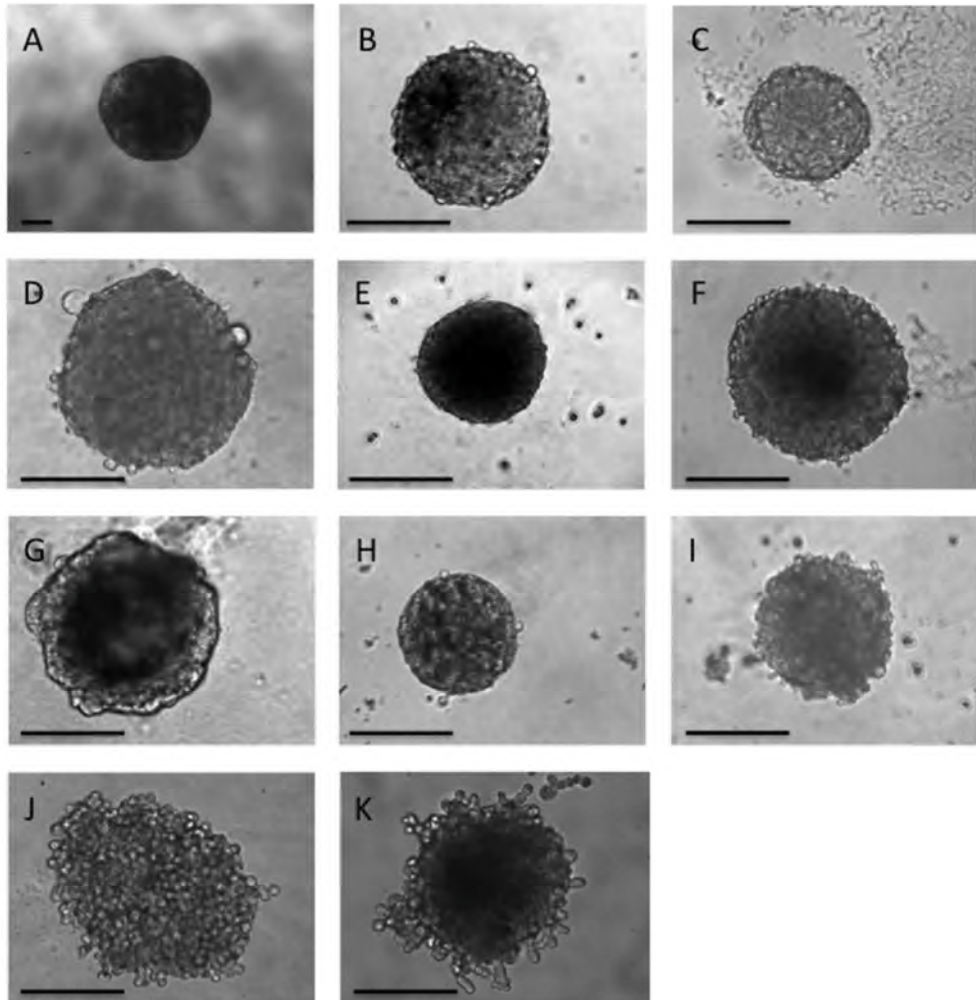


Figure 2

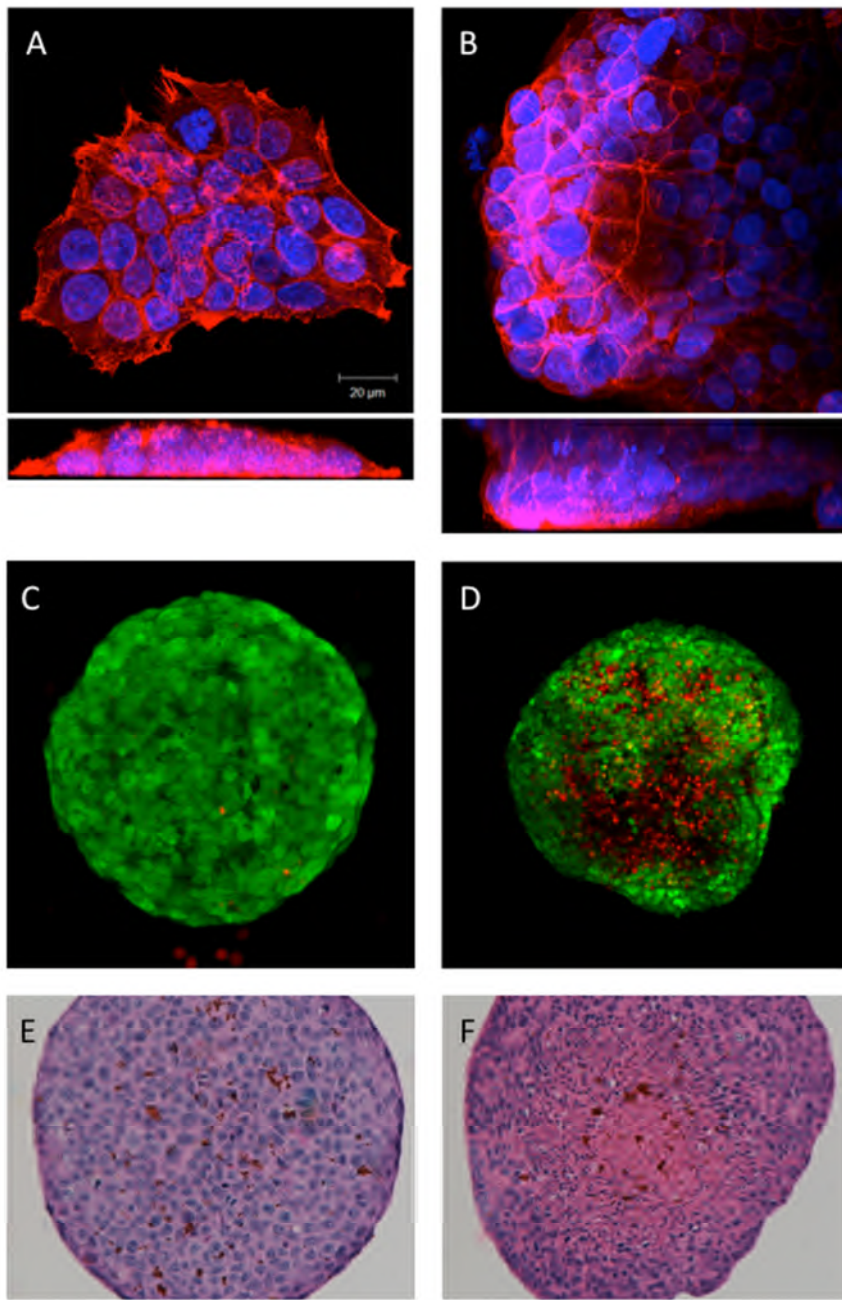


Figure 3

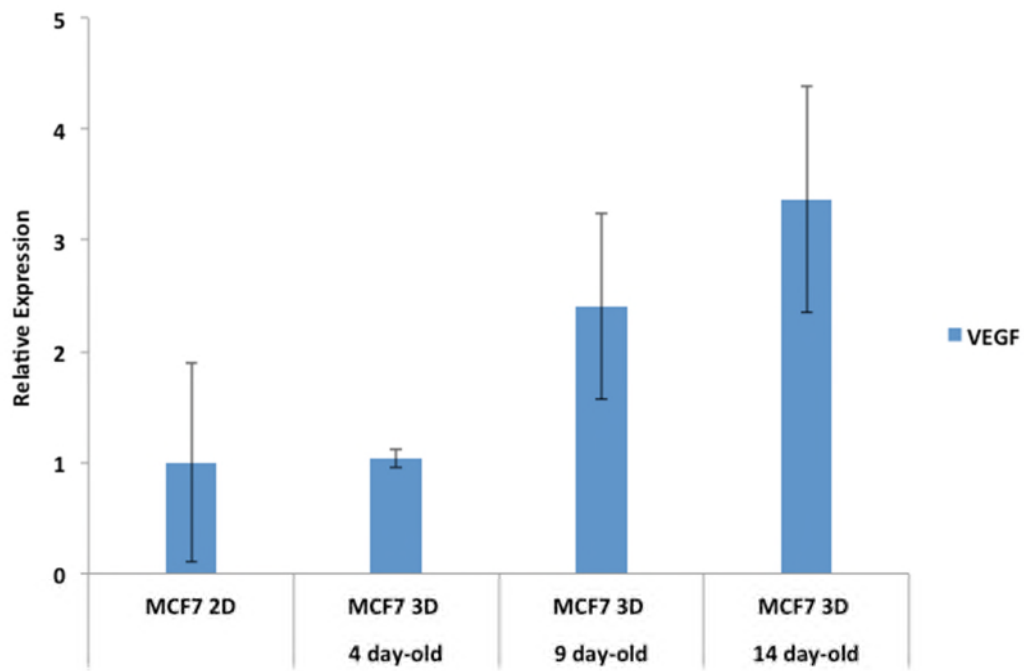


Figure 4

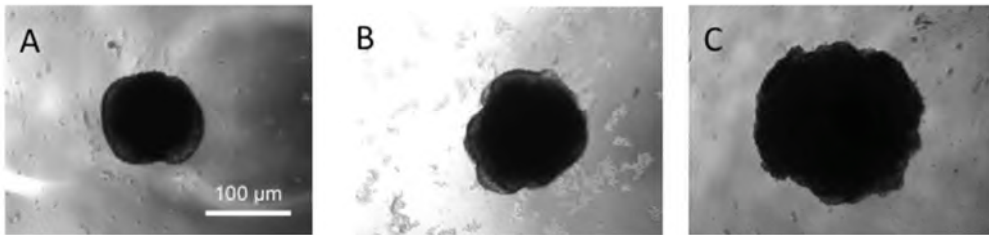


Figure 5

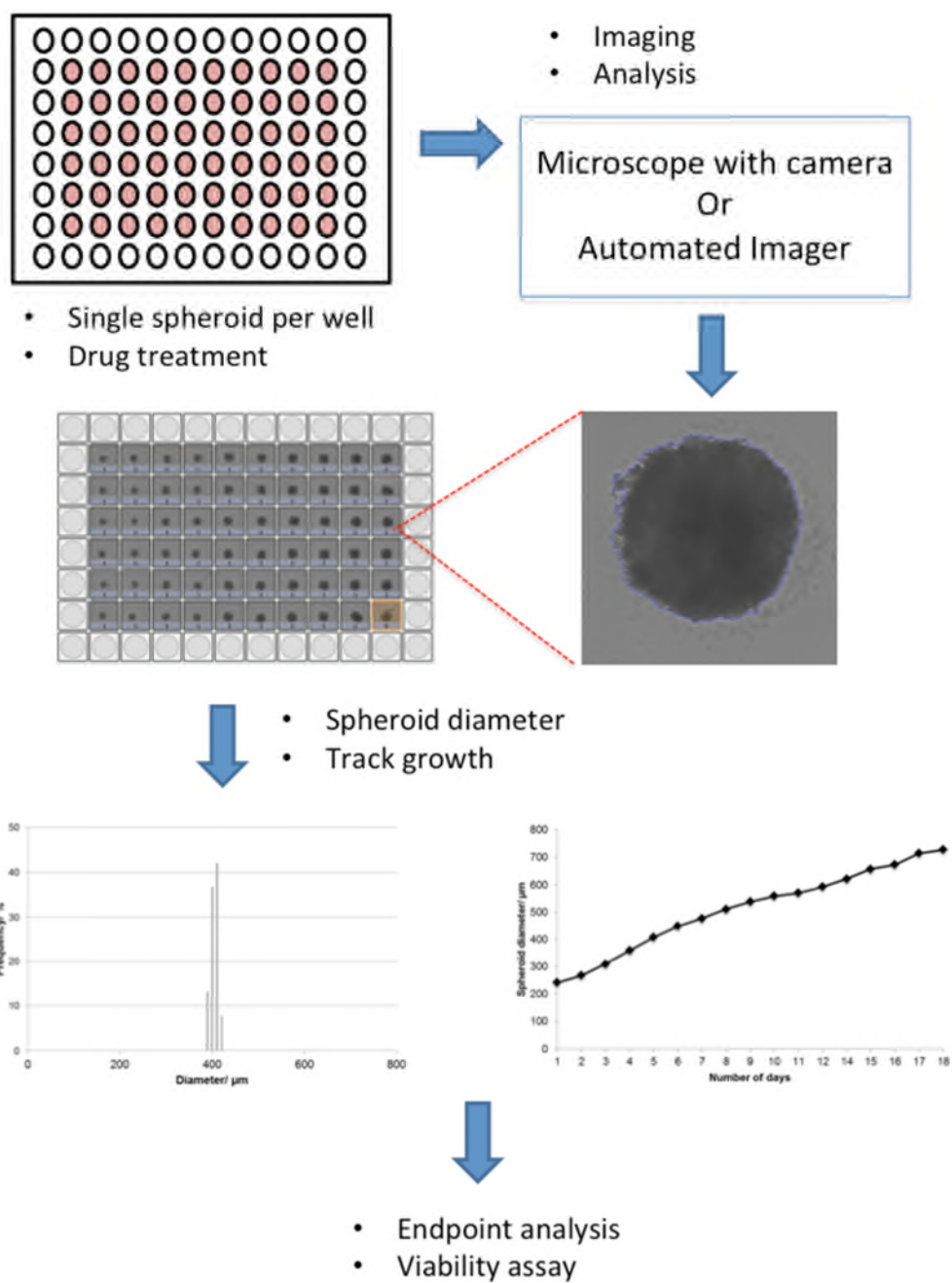


Figure 6

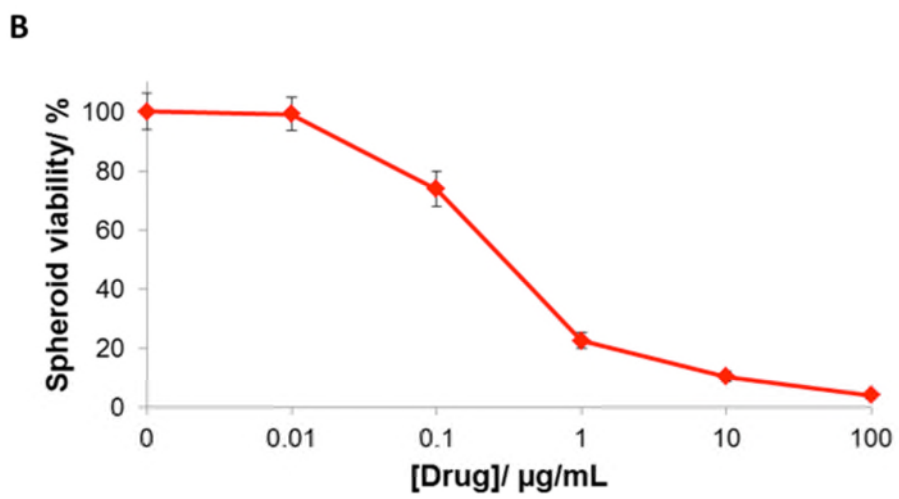
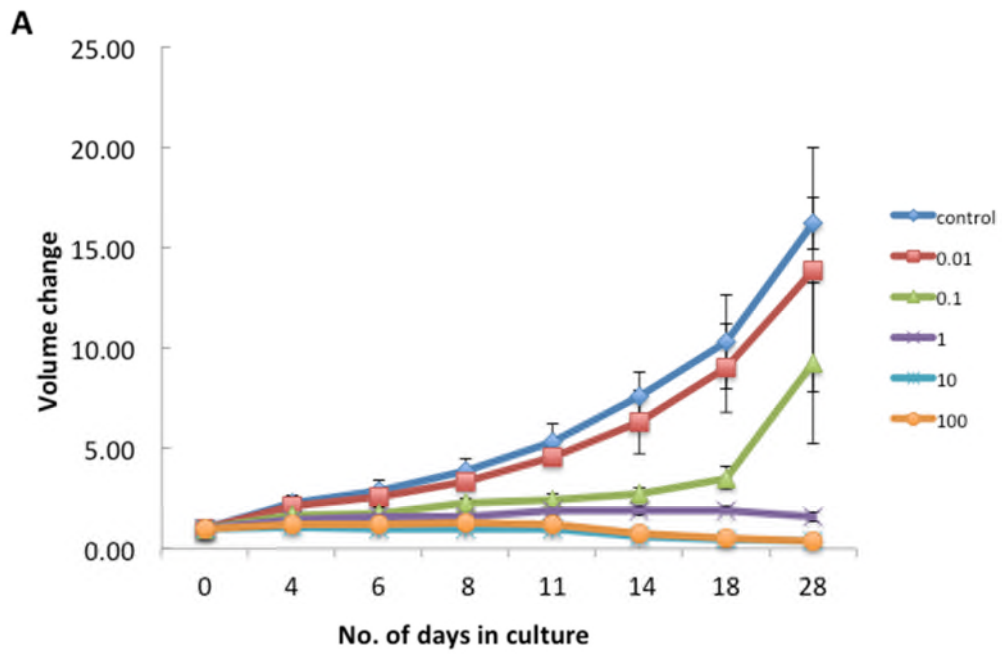


Figure 7